Constraining new physics in B_s^0 meson mixing

Wouter Hulsbergen

The Netherlands institute for sub-atomic physics (Nikhef)

June 2013

Abstract

Neutral mesons exhibit a phenomenon called flavour mixing. As a consequence of a second order weak process the flavour eigenstates corresponding to the meson and its anti-meson are superpositions of two mass eigenstates. A meson produced in a flavour state changes into an anti-meson and back again as a function of time. Such flavour oscillations are considered sensitive probes of physics beyond the Standard Model. In this brief review I summarize the status of experimental constraints on mixing parameters in the B_s^0 meson system.

To appear in Mod. Phys. Lett. A.

1 Introduction

Quarks are the fundamental fermions that make up baryonic matter in the universe. In the Standard Model (SM) of elementary particles quarks come in six flavours, organized in three families,

$$\left(\begin{array}{c} \mathrm{up}\;(u)\\ \mathrm{down}\;(d) \end{array}\right) \quad \left(\begin{array}{c} \mathrm{charm}\;(c)\\ \mathrm{strange}\;(s) \end{array}\right) \quad \left(\begin{array}{c} \mathrm{top}\;(t)\\ \mathrm{beauty}\;(b) \end{array}\right) \ .$$

The up-type quarks (top row) have charge $\frac{2}{3}e$ while the down-type quarks (bottom row) have charge $-\frac{1}{3}e$. We denote these quarks with the symbol q_i where the index refers to the flavour. Quarks have mirror images called anti-quarks, which we denote with the symbol \bar{q}_i . Their physical properties are identical to those of the quarks, except that they have opposite quantum numbers for charge and flavour.

In the SM only the charged weak interaction, mediated by the charged W boson, can change quark flavour. It leads to couplings of the form $u \to W^+ d$, where the transition is always between an up-type and a down-type quark. The strength of the coupling is proportional to the weak coupling constant and to the elements of a complex unitary matrix that is called the Cabibbo-Kobayashi-Maskawa (CKM) matrix and is usually represented as

$$V_{\rm CKM} = \begin{pmatrix} V_{ud} & V_{us} & V_{ub} \\ V_{cd} & V_{cs} & V_{cb} \\ V_{td} & V_{ts} & V_{tb} \end{pmatrix} .$$
(1)

The off-diagonal elements of $V_{\rm CKM}$ are responsible for transitions between the three quark families. They are small compared to the on-diagonal elements, which are all close to unity. For three generations the $V_{\rm CKM}$ matrix can be parametrized by four real numbers, namely three rotation angles and one phase. The non-zero value of this phase is the single source of CP violation (a difference between matter and anti-matter) in the quark sector of the SM.¹ In 2008 Kobayashi and Maskawa were awarded a Nobel prize for their explanation of CP violation with this mechanism. In a sense they predicted the existence of the charm, beauty and top quark well before their discovery.

Mesons are bound states of a quark q_i and an anti-quark \bar{q}_j . (The top quark does not appear in bound states as it decays too quickly.) The lowest-energy states of mesons with quarks with different flavour — those with no net orbital angular momentum — can only decay via the weak interaction and are therefore meta-stable, with lifetimes in the range of 10^{-13} to 10^{-7} seconds.

If the $q_i \bar{q}_j$ combination is neutral, a phenomenon occurs that is called *mixing*: the mass eigenstates of such mesons are quantum-mechanical superpositions of the flavour eigenstate $q_i \bar{q}_j$ and the *CP*-conjugate flavour eigenstate $\bar{q}_i q_j$. As a result a meson created in a $q_i \bar{q}_j$ state may decay as a $\bar{q}_i q_j$ state with a probability that changes as a function of time. Table 1 lists the average decay times and oscillation period of the four mesons that are subject to mixing.

Table 1: Neutral charm and beauty mesons with approximate mass, lifetime and mixing period.² In the K^0 system there are two states with very different lifetime. Below only the lifetime of the short-lived state, the K_{short} , is shown.

name	quark content	$\mathrm{mass}/\mathrm{MeV}$	lifetime/ps	oscillation period/ps
K^0	$s ar{d}$	498	90	1190
D^0	$car{u}$	1865	0.41	440
B_d^0	$dar{b}$	5280	1.5	12.4
$\frac{B_d}{B_s^0}$	$sar{b}$	5367	1.5	0.36

The transition amplitude that governs neutral meson mixing is an example of a so-called *flavour-changing neutral current* (FCNC). In the SM neutral meson mixing occurs via a second order weak amplitude, depicted for B_s^0 mesons in Fig. 1. As such processes are heavily suppressed,³ they are considered to be very sensitive to contributions from physics beyond the SM. Mixing of B_s^0 mesons is particularly interesting for two reasons. First, the heavy mass of the *b* quark allows for relatively reliable calculations of mixing parameters. Second, it is sensitive to new contributions in $b \to s$ transitions, which are until now relatively poorly constrained.

The subject of this review is the status of experimental constraints on B_s^0 mixing. We start with a summary of the neutral meson mixing phenomenology in order to introduce the experimental observables and SM predictions. Subsequently, experimental techniques and existing measurements are discussed. We finish with a conclusion and a brief outlook.

$$B_{s}^{0} \qquad \begin{array}{c|c} b \\ W \\ s \\ t, c, u \\ s \\ t, c, u \\ b \end{array} \qquad \begin{array}{c|c} s \\ W \\ B_{s}^{0} \\$$

Figure 1: Leading order diagrams for neutral meson mixing in the SM.

2 Beauty mixing phenomenology in a nutshell

Excellent pedagogical introductions to neutral meson mixing can be found in textbooks⁴, recent reviews^{5,6} and lecture notes.^{7,8} An up-to-date review of experimental constraints on B meson mixing can also be found in the PDG.⁹ The following discussion applies to neutral mesons of any kind. However, we shall denote the flavour eigenstate with the symbol B^0 for beauty meson and use numerical estimates that apply to B_s^0 and B_d^0 .

2.1 Time-evolution of the B^0 - \overline{B}^0 system

Consider the wave function $B^0(t)$ for a neutral meson that is the superposition of flavour eigenstates B^0 and \overline{B}^0 . The time-evolution of its projections into flavour eigenstates is given by a Schrödinger equation

$$i\frac{\mathrm{d}}{\mathrm{d}t} \left(\begin{array}{c} \langle B^0 | B(t) \rangle \\ \langle \overline{B}^0 | B(t) \rangle \end{array} \right) = \left(\begin{array}{c} H_{11} & H_{12} \\ H_{21} & H_{22} \end{array} \right) \left(\begin{array}{c} \langle B^0 | B(t) \rangle \\ \langle \overline{B}^0 | B(t) \rangle \end{array} \right).$$
(2)

Since the meson decays and we do not consider the wave function of final states, the Hamiltonian H is not hermitian. However, like any other complex matrix, it can be decomposed in terms of two hermitian matrices, which we label by M and Γ ,

$$H = M - \frac{i}{2}\Gamma.$$
 (3)

Since M and Γ are hermitian, their diagonal elements are real and we have $M_{21} = M_{12}^*$ and $\Gamma_{21} = \Gamma_{21}^*$. *CPT* invariance requires $M_{11} = M_{22}$ and $\Gamma_{11} = \Gamma_{22}$. Ignoring for the moment the interference with phases in the final state, the common phase of B^0 and \overline{B}^0 is arbitrary such we can choose either the phase of M_{12} or Γ_{12} and only their phase difference matters. Consequently, the mixing can be parametrized by five real parameters, which are conventionally chosen to be

$$M_{11}, \quad \Gamma_{11}, \quad |M_{12}|, \quad |\Gamma_{12}| \quad \text{and} \quad \phi_{12} = \arg\left(-\frac{M_{12}}{\Gamma_{12}}\right).$$
 (4)

The mass M_{11} is determined by the quark masses and strong interaction binding energy. In the *B* system it is about 5 GeV and more than ten orders of magnitude larger than the size of the other elements, which all involve the weak interaction.

The time-evolution of the meson-anti-meson system is described in terms of the eigenstates of the Hamiltonian. The two mass eigenstates can be written as linear combinations of the flavour eigenstates,

$$|B_L\rangle = p |B^0\rangle + q |\overline{B}^0\rangle |B_H\rangle = p |B^0\rangle - q |\overline{B}^0\rangle$$
(5)

where the subscripts H and L stand for 'heavy' and 'light', q and p are complex numbers and normalization requires $|p|^2 + |q|^2 = 1$. For q/p = 1 the mass eigenstates correspond to CP eigenstates. On the other hand, if $q/p \neq 1$, CP is not conserved in the time-evolution of the $B^0 - \overline{B}^0$ system.

The eigenvalues corresponding to the heavy and light states are written as

$$\omega_{L,H} \equiv m_{L,H} - \frac{i}{2}\Gamma_{L,H} \tag{6}$$

and are usually recast in terms of the observables

$$m \equiv \frac{1}{2} (m_H + m_L) = M_{11} \qquad \Gamma \equiv \frac{1}{2} (\Gamma_H + \Gamma_L) = \Gamma_{11}$$

$$\Delta m \equiv m_H - m_L \qquad \Delta \Gamma \equiv \Gamma_L - \Gamma_H . \qquad (7)$$

Note that the two eigenstates can have both different mass and lifetimes. By convention the heavy and light solutions are labeled such that Δm is positive. Using that in the *B* meson systems $|\Gamma_{12}| \ll |M_{12}|$ one finds⁷

$$\Delta M \approx 2|M_{12}|$$
 and $\Delta \Gamma \approx 2|\Gamma_{12}|\cos\phi_{12}$. (8)

As we shall see later, Δm can be measured by observing an asymmetry in the decay time distribution of B^0 and \overline{B}^0 , while $\Delta\Gamma$ is obtained by combining lifetime measurements of decays to final states with different CP content.

The ratio q/p can be written as

$$\frac{q}{p} = e^{-i\phi_M} \sqrt{\frac{|M_{12}| + \frac{i}{2}|\Gamma_{12}|e^{i\phi_{12}}}{|M_{12}| + \frac{i}{2}|\Gamma_{12}|e^{-i\phi_{12}}}}$$
(9)

where $\phi_M \equiv \arg(M_{12})$. For $\phi_{12} \neq 0, \pi$ the absolute value of q/p is different from unity, a case we refer to as *CP violation in mixing*. Using $|\Gamma_{12}| \ll |M_{12}|$ we have for the difference of $|q/p|^2$ with one

$$1 - \left|\frac{q}{p}\right|^2 \approx \left|\frac{\Gamma_{12}}{M_{12}}\right| \sin \phi_{12} \tag{10}$$

Since the time-evolution of the mass eigenstates follows $|B_{H,L}(t)\rangle = \exp(-i\omega_{H,L}) |B_{H,L}(0)\rangle$, the time-evolution of a B^0 meson produced in a B^0 or \overline{B}^0 flavour eigenstate at t = 0 can now be written as

$$|B^{0}(t)\rangle = g_{+}(t) |B^{0}\rangle + \frac{q}{p} g_{-}(t) |\overline{B}^{0}\rangle$$

$$|\overline{B}^{0}(t)\rangle = g_{+}(t) |\overline{B}^{0}\rangle + \frac{p}{q} g_{-}(t) |B^{0}\rangle$$
(11)

with the functions $g_{\pm}(t)$ defined as

$$g_{\pm}(t) = \frac{1}{2} \left(e^{-i\omega_L} \pm e^{-i\omega_H} \right) \tag{12}$$

The probability to observe at time t the decay into a state with a flavour that is the same as (plus sign) or opposite to (minus sign) the flavour with which is was produced is then proportional to

$$|g_{\pm}(t)|^2 = \frac{e^{-\Gamma t}}{2} \left[\cosh\left(\frac{1}{2}\Delta\Gamma t\right) \pm \cos\left(\Delta m t\right) \right], \tag{13}$$

while the time-integrated oscillation probability is given by

$$\chi = \frac{1}{2} \frac{4\Delta m^2 + \Delta\Gamma^2}{4\Delta m^2 + \Gamma^2}.$$
(14)

2.2 Including decay amplitudes

The formalism above only describes the time-evolution of the $B^0 - \overline{B}^0$ system and not yet the decay to an observable final state f. For a given final state we define two transition amplitudes

$$A_f \equiv \langle f | \mathcal{H} | B^0 \rangle$$
 and $\overline{A}_f \equiv \langle f | \mathcal{H} | \overline{B}^0 \rangle$, (15)

where \mathcal{H} is the weak interaction Hamiltonian responsible for the decay. For a meson produced in an initial flavour eigenstate B^0 the decay width to the final state f receives two contributions, namely one from A_f and another one from \overline{A}_f where the B^0 first oscillated to a \overline{B}^0 , schematically depicted in Fig. 2. The partial decay rate can be written as¹⁰

$$\Gamma_{B\to f}(t) = |A_f|^2 \left(1 + |\lambda_f|^2\right) \frac{e^{-\Gamma t}}{2} \left[\cosh\left(\frac{1}{2}\Delta\Gamma t\right) + D_f \sinh\left(\frac{1}{2}\Delta\Gamma t\right) + C_f \cos\left(\Delta m t\right) - S_f \sin\left(\Delta m t\right)\right]$$
(16)

where we defined

$$\lambda_f = \frac{q}{p} \frac{A_f}{A_f} \tag{17}$$

and 1

$$C_{f} \equiv \frac{1 - |\lambda_{f}|^{2}}{1 + |\lambda_{f}|^{2}} \qquad S_{f} \equiv \frac{2\Im(\lambda_{f})}{1 + |\lambda_{f}|^{2}} \qquad D_{f} \equiv -\frac{2\Re(\lambda_{f})}{1 + |\lambda_{f}|^{2}}.$$
 (18)

The decay rate for $\overline{B}^0 \to f$ is obtained from this expression by changing the sign of C_f and S_f and multiplying by an overall factor $|p/q|^2$. Similar expressions can be derived for the decay of B^0 to the CP conjugate state \overline{f} by a suitable redefinition of λ . It is important to note that, in contrast to M_{12} , Γ_{12} and the elements of the CKM matrix, λ_f is a phase convention-independent physical observable.¹¹

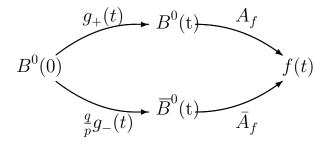


Figure 2: Graphical illustration of the interference of two amplitudes leading to time-dependent CP violation in decay of a neutral meson to a CP eigenstate.

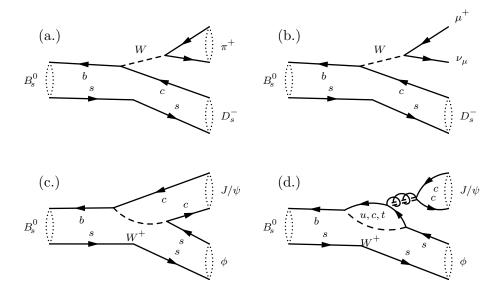


Figure 3: Leading order Feynman diagrams for a few B_s^0 decay modes relevant for this review.

We now consider two cases relevant for this review. Flavour-specific final states are final states for which $|\bar{A}_f| \ll |A_f|$ such that $\lambda \simeq 0$. Important examples are the tree-level transitions $B_s^0 \to D_s^+ \pi^-$ and $B_s^0 \to D_s^+ \mu^- \bar{\nu}_{\mu}$ shown in Fig. 3. Under the assumption of no *CP*-violation in mixing (|q/p| = 1) and no *CP*-violation in the decay $(|A_f| = |\bar{A}_{\bar{f}}|)$, we can derive the following expression for the so-called time-dependent oscillation (or 'mixing') probability,

$$A_{\rm mix}(t) \equiv \frac{\left(\Gamma_{B^0 \to f} + \Gamma_{\bar{B}^0 \to \bar{f}}\right) - \left(\Gamma_{B^0 \to \bar{f}} + \Gamma_{\bar{B}^0 \to f}\right)}{\left(\Gamma_{B^0 \to f} + \Gamma_{\bar{B}^0 \to \bar{f}}\right) + \left(\Gamma_{B^0 \to \bar{f}} + \Gamma_{\bar{B}^0 \to f}\right)} = \frac{\cos \Delta m t}{\cosh \frac{1}{2} \Delta \Gamma t} .$$
(19)

The two terms in the definition of the asymmetry are usually called the 'unmixed' and 'mixed' contribution, respectively. In section 4.1 we discuss measurements of the oscillation probability with flavour-specific final states.

¹There exist alternative notations for these three quantities, in particular $A_f^{\text{dir}} \equiv C_f$, $A_f^{\text{mix}} \equiv -S_f$ and $A_f^{\Delta\Gamma} \equiv D_f$. However, be aware that different conventions are used regarding the signs of these quantities.

Alternatively, dropping the requirement on q/p we can form the following CP asymmetry

$$a_{\rm fs} \equiv \frac{\Gamma_{B^0 \to \bar{f}} - \Gamma_{\bar{B}^0 \to f}}{\Gamma_{B^0 \to \bar{f}} + \Gamma_{\bar{B}^0 \to f}} = \frac{1 - |q/p|^4}{1 + |q/p|^4}$$
(20)

which is notably time-independent. This asymmetry is called the flavour-specific or semi-leptonic asymmetry. (HFAG denotes this quantity with $\mathcal{A}_{\rm sl}$.) Note the particle and anti-particle labels in this definition: both are 'mixed' contributions. In the *B* meson system |q/p| is close to one. To translate the measurement of $a_{\rm fs}$ into constraints on ϕ_{12} one often uses the relation

$$a_{\rm fs} \approx 1 - |q/p|^2 \approx \frac{\Delta\Gamma}{\Delta m} \tan \phi_{12}$$
 (21)

One way to measure $a_{\rm fs}$ is by counting the number of positive like-sign and negative like-sign muon pairs in events in which both b quarks decay semi-leptonically,

$$a_{\rm fs} = \frac{N(\mu^+\mu^+) - N(\mu^-\mu^-)}{N(\mu^+\mu^+) + N(\mu^-\mu^-)}$$
(22)

As we shall see in section 4.4 the measurement of flavour-specific asymmetry with semi-leptonic and $B \to D\pi$ decays provides the best constraints on |q/p| in the B_s^0 system.

Next we consider decays to final states f that are (mixtures of) CP eigenstates, most notably $B_d^0 \to J/\psi K_S^0$ and $B_s^0 \to J/\psi \phi$. Figure 3c and d show tree- and penguin-level contributions to the $B_s^0 \to J/\psi \phi$ amplitude. If a final state f is accessible to both the B^0 and the \overline{B}^0 meson, then interference between decay via mixing and decay without mixing gives rise to CP-violation. More specifically, if all contributing decay amplitudes carry the same weak phase, then the decay amplitude ratio can be written as $A_f/\overline{A}_f = \eta_f e^{2i\phi_{\rm D}}$, where $\eta_f = \pm 1$ is the CPeigenvalue of the final state and $\phi_{\rm D} = \arg(A_f)$. If one further assumes that CPviolation in mixing is small $(|q/p| \approx 1)$, then

$$\lambda = \eta_f e^{-i\phi_M} e^{2i\phi_D} \,. \tag{23}$$

where the phase $\phi_M \equiv \arg(M_{12})$ enters via Eq. 9. The time-dependent *CP*-asymmetry can then be written as

$$A_{CP}(t) \equiv \frac{\Gamma_{B^0 \to f} - \Gamma_{\bar{B}^0 \to f}}{\Gamma_{B^0 \to f} + \Gamma_{\bar{B}^0 \to f}} = \frac{\eta_f \sin \phi_f \sin \Delta m t}{\cosh \frac{1}{2} \Delta \Gamma t - \eta_f \cos \phi_f \sinh \frac{1}{2} \Delta \Gamma t}.$$
 (24)

where we introduced the commonly used CP violating phase

$$\phi_f \equiv -\arg(\lambda_f) = \phi_M - 2\phi_D \,. \tag{25}$$

By measuring the amplitude of the sinusoid in the time-dependent asymmetry we constrain the phase ϕ_f . Since this phase is related to the phase of M_{12} , the CP asymmetry is a direct probe of new contributions to M_{12} .

For decays to CP-eigenstates with a single contributing amplitude the phase ϕ_f can be directly expressed in terms of elements of V_{CKM} . In particular, we have for the so-called 'golden modes', that occur through a tree-level $b \to c\bar{c}s$ transition,

$$\begin{array}{lll}
B_d^0 \to J/\psi K_S^0 & : & \phi_d^{ccs} = 2\beta \\
B_s^0 \to J/\psi \phi & : & \phi_s^{ccs} = -2\beta_s
\end{array}$$
(26)

where the CKM phases β and β_s are defined by¹²

$$\beta \equiv \arg\left(-\frac{V_{cd}V_{cb}^*}{V_{td}V_{tb}^*}\right) \quad \text{and} \quad \beta_s \equiv \arg\left(-\frac{V_{ts}V_{tb}^*}{V_{cs}V_{cb}^*}\right) \,. \tag{27}$$

We discuss the measurement of $\phi_s^{c\bar{c}s}$ with $B_s^0 \to J/\psi\phi$ and $B_s^0 \to J/\psi f^0$ decays in section 4.2.

Finally, we consider lifetimes. The 'untagged' decay time distribution for a final state f can be obtained from Eq. 16 by setting C = S = 0. The average decay time (sometimes called the 'effective lifetime') is given by¹³

$$\tau_f = \frac{(1 - D_f)/\Gamma_{\rm L}^2 + (1 + D_f)/\Gamma_{\rm H}^2}{(1 - D_f)/\Gamma_{\rm L} + (1 + D_f)/\Gamma_{\rm H}} = \frac{1}{\Gamma} \frac{1 + 2D_f y + y^2}{(1 - y^2)(1 + D_f y)}$$
(28)

where D_f was defined above and $y = \Delta \Gamma/2\Gamma$. For flavour-specific modes $D_f = 0$ while for decays to CP-eigenstates with a single contribution amplitude it is $D_f = -\eta_f \cos \phi_f$. In section 4.3 we shall discuss constraints on Γ_s and $\Delta \Gamma_s$ from various final states.

2.3 Standard Model predictions

In the SM the computation of B^0 mixing parameters is performed by evaluating the amplitudes corresponding to the box diagrams shown in Fig. 1. Since quarks are not free particles, these amplitudes need to be corrected for hadronization effects. The calculations have been the cumulative effort of many people, over a period of over twenty years. (See Refs. 14, 15, 16, 17 and references therein.)

The latest complete computation of the mixing observables can be found in Ref. 16, with an update of numerical estimates in Ref. 18. The value of M_{12} is obtained from a calculation of the box diagram in Fig. 1 with a virtual top quark in the loop. The result can be expressed as¹⁶

$$M_{12}^{q} = \frac{G_{F}^{2} m_{W}^{2}}{12\pi^{2}} \left(V_{tq}^{*} V_{tb} \right)^{2} S_{0} \left(\frac{m_{t}^{2}}{m_{W}^{2}} \right) \eta_{B} \hat{B}_{B_{q}} f_{B_{q}}^{2} m_{B_{q}}$$
(29)

The part of this expression to the left of η_B follows from a computation of the box diagram for free quarks in perturbation theory. It depends on parameters of the SM, such as the Fermi coupling constant G_F , the CKM matrix elements V_{ij} and the top quark and W boson masses. The function $S_0(x)$ is a known kinematic function, called the Inami-Lim function,¹⁹ and $S_0(m_t^2/m_W^2) \approx 2.3$. The numerical factor $\eta_B \approx 0.55$ accounts for QCD corrections. The factors to its right account for the fact that the quarks are confined in hadrons. While the B meson mass m_B is just taken from measurements, the decay constant f_B and the bag factor \hat{B}_B are computed using Lattice gauge theory. (For a recent review see Ref. 20). The uncertainty on the prediction of M_{12} is dominated by the theoretical uncertainty in $\hat{B}_B f_B^2$.

The computation of Γ_{12} involves the evaluation of the box diagram with 'onshell' internal quarks, the dominant contribution coming from the $b \to c\bar{c}s$ transition. Since the latter is a tree-level transition, Γ_{12} is expected to be less sensitive to new physics than M_{12} is. It can be written as²¹

$$\Gamma_{12}^{q} = -\frac{G_{F}^{2}m_{b}^{2}}{8\pi^{2}} \left[\left(V_{tq}^{*}V_{tb} \right)^{2} + V_{tq}^{*}V_{tb}V_{cq}^{*}V_{cb}\mathcal{O}\left(\frac{m_{c}^{2}}{m_{b}^{2}}\right) + \left(V_{cq}^{*}V_{cb} \right)^{2}\mathcal{O}\left(\frac{m_{c}^{2}}{m_{b}^{2}}\right) \right] \eta_{B}' \hat{B}_{B_{q}}f_{B_{q}}^{2}m_{B_{q}} \quad (30)$$

where the QCD correction factor η'_B is of order unity. Note that Γ_{12} is proportional to $\hat{B}_B f_B^2$ as well, such that predictions for the ratio Γ_{12}/M_{12} have smaller theoretical uncertainty than those for M_{12} and Γ_{12} separately. Furthermore, since the ratio is proportional to $m_b^2/m_W^2 \approx 0.005$, we expect $|\Gamma_{12}| \ll |M_{12}|$ in the SM.

The only source of a complex phase in the expressions for M_{12} and Γ_{12} are the CKM matrix elements. The size of the CKM matrix elements in Eq. 30 is such that the term proportional to $(V_{tq}^*V_{tb})$ dominates. Consequently, taking into account the minus sign in front of Γ_{12} , the phase difference between M_{12} and Γ_{12} is approximately π and ϕ_{12} is small in the SM. This also implies, by virtue of Eq. 8, that $\Delta\Gamma$ is positive: the heavier mass eigenstate has the smaller decay width.

The SM does not predict the size of coupling constants, quark masses and the elements of the CKM matrix. Consequently, theoretical predictions of mixing observables always rely on other measurements to determine the SM parameters. The latter are usually obtained from global fits to the experimental data that do not include the mixing observables themselves.^{22,23}

	B_d^0	B_s^0		
ϕ_{12} [rad.]	-0.075 ± 0.024	0.004 ± 0.001		
$\Delta\Gamma[\mathrm{ps}^{-1}]$	$(2.7 \pm 0.5) \cdot 10^{-3}$	0.087 ± 0.021		
$\Delta m [{\rm ps}^{-1}]$	0.555 ± 0.073 *	17.3 ± 2.6		
a_{fs}	$-(4.1\pm0.6)\cdot10^{-4}$	$(1.9 \pm 0.3) \cdot 10^{-5}$		
$\phi^{c\bar{c}s}$ [rad.]	$0.84\pm0.05^*$	$-0.036 \pm 0.002^{*}$		

Table 2: Predictions for mixing observables taken from Ref. 18, except for (*), taken from Ref. 24.

The SM predictions are summarized in table 2. Note that, for some results in the table, experimental measurements are used to reduce the uncertainties. For example, the ratio $\Delta\Gamma_d/\Delta m_d$ has smaller uncertainties than $\Delta\Gamma_d$ by itself. Consequently, for the prediction of $\Delta\Gamma_d$, the measured value of Δm_d was used.

Likewise, the computation of Δm_s requires an estimate of V_{ts} . Since the computation of the perturbative parts of the amplitude is identical for B_s^0 and B_d^0 , the

ratio $\Delta m_s / \Delta m_d$ can be written as

$$\frac{\Delta m_s}{\Delta m_s} = \xi^2 \frac{m_{B_s^0}}{m_{B_d^0}} \left| \frac{V_{ts}}{V_{td}} \right|^2, \tag{31}$$

where the so-called SU(3)-breaking ratio is defined as

$$\xi \equiv \frac{f_{B_s^0} \sqrt{\hat{B}_{B_s^0}}}{f_{B_d^0} \sqrt{\hat{B}_{B_d^0}}}.$$
(32)

The computation of ξ with lattice QCD has meanwhile reached a precision of a few percent.²⁵ With these expressions one can either test the prediction of Δm_s by using other constraints to estimate V_{ts}/V_{td} (as was done to obtain the results in the table), or use the measurement of $\Delta m_s/\Delta m_d$ to obtain a precise determination of V_{ts}/V_{td} .

There exists no SM predictions for the B meson masses as these are essentially determined by the quark masses. Although the total decay widths cannot be computed reliably either, their ratio is well constrained and is almost unity in the SM^{26,27,18}

$$0 \leq \frac{\Gamma_s}{\Gamma_d} - 1 \leq 4 \cdot 10^{-4}.$$
 (33)

As we shall see, this prediction agrees well with experimental data. Since uncertainties in this computation rely on similar assumptions as those for Γ_{12} the agreement with data is sometimes taken as a sign that the computation of Γ_{12} is reliable.

The interpretation of the observable ϕ_f in $B_d^0 \to J/\psi K_S^0$ and $B_s^0 \to J/\psi \phi$ decays in terms of the tree-level quantity $\phi^{c\bar{c}s}$ ignores a small contribution from penguin decays with a different weak phase, such as depicted in Fig. 3d. These contributions may change ϕ_f by up to a few degrees and can be constrained using measurements from other decay modes that are related by flavour symmetries.²⁸

2.4 Beyond the Standard Model

Many viable TeV-scale extensions of the SM predict new flavour-changing neutral couplings, which in turn affect the mixing parameter M_{12} and for instance the rare decay $B_s^0 \to \mu^+ \mu^-$. As different models affect these quantities differently, it is through a combination of flavour measurements that one hopes to identify the correct theory. (For an overview, see Ref. 29.)

The effect of new contributions to M_{12} is usually parametrized by introducing a complex parameter Δ_q such that 30,31,16

$$M_{12}^q \equiv M_{12}^{q,\text{SM}} \Delta_q \tag{34}$$

If the magnitude of Δ_q differs from unity, this affects the observed mixing frequency. If its phase differs from zero, this affects ϕ_{12} and thereby $\Delta\Gamma$, $a_{\rm fs}$ and the CP phases extracted from measurements of time-dependent CP violation. For recent evaluations on constraints on Δ_q from B_s^0 mixing measurements, see for instance Ref. 32. A recent overview of implications and relations to other flavour physics observables can be found in Refs. 33, 34.

3 Experimental facilities and techniques

The discovery of the Υ (a $b\bar{b}$ bound state) in decays to $\mu^+\mu^-$ by Lederman and collaborators in 1977³⁵ marks the onset of beauty-quark physics. Although the *b* quark was first found in a fixed-target experiment, most experimental knowledge comes from two other types of facilities. The first are e^+e^- colliders with a centre-of-momentum energy tuned to the $\Upsilon(4S)$ resonance, a $b\bar{b}$ state with a mass just above the $B_d^0 \bar{B}_d^0$ and B^+B^- threshold. These facilities are usually called e^+e^- *B*-factories. The $b\bar{b}$ cross-section at the $\Upsilon(4S)$ is about 1 nb. The fact that this is about one fourth of the total hadronic cross-section at this energy allows for very clean studies of *B* meson properties.

Early e^+e^- *B*-factories (DORIS, CESR) were operated with symmetric energy beams. As the $\Upsilon(4S)$ resonance is just above the $B-\overline{B}$ meson threshold, $B-\overline{B}$ pairs are produced practically at rest in the centre-of-momentum system. Investigations at $\Upsilon(4S)$ facilities took a big step forward with the advance of the asymmetricenergy e^+e^- colliders KEKB and PEP-II. These accelerators operated at the $\Upsilon(4S)$ resonance as well, but with a positron beam energy roughly half that of the electron beam. The resulting *B*-meson boost, approximately $\gamma\beta = 0.5$ at both colliders, allows for a measurement of the decay time with sufficient precision to resolve B_d^0 flavour oscillations. Thanks to the unprecedented instantaneous luminosity, the asymmetric *B*-factories have collected samples of approximately $10^9 \ B-\overline{B}$ events. The next generation $e^+e^- \ B$ -factory, super-KEK, is expected to start operation in 2015, allowing for an increase in statistics with another factor 50.

Beauty hadrons have also been extensively studied at high-energy colliders, both at e^+e^- machines (SLD, LEP) and at hadron colliders (SPS, Tevatron, LHC). At these facilities one profits from a larger cross-section, albeit at the expense of a poorer signal-to-background ratio. For example, with a cross-section of about $300\,\mu$ b, a total of approximately $10^{12} b\bar{b}$ pairs have been produced in collisions in the first LHC run (2010-2012). However, these need to be extracted from an inelastic background that is a factor 200 larger. As only a fraction of events can be written to permanent storage, the experiments rely on signatures such as $J/\psi \to \mu^+\mu^-$ decays, detached muons or detached high- p_{\perp} hadrons to select the events of interest.

Besides the larger cross-section the high-energy facilities have two advantages: First, all species of b quark hadrons are produced, not only the B_d^0 and B_u^{\pm} mesons found at the $\Upsilon(4S)$ resonance. Approximately 10% of all b (\bar{b}) quarks hadronize into \bar{B}_s^0 (B_s^0) mesons. Although studies of B_s^0 mesons have been performed by operating at higher $e^+e^- \to \Upsilon$ resonances, conditions at these higher resonances are not favourable enough to produce competitive B_s^0 samples. Second, thanks to the much larger b quark boost, the decay time resolution in high energy colliders far exceeds that at the *B*-factories. As we shall see below, a good decay time resolution is essential to resolve B_s^0 flavour oscillations. Consequently, the study of B_s^0 oscillations is (for now) only performed at high-energy colliders.

Figure 4 shows schematically the production and decay of a neutral B meson in a high-energy collider experiment. Due to the finite decay time of the B, its decay vertex is displaced with respect to the collision point. Silicon vertex trackers

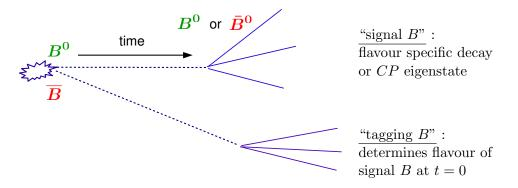


Figure 4: Schematic representation of the production and decay of a B meson in a high-energy collision.

have sufficient position accuracy to measure the decay length L, which is typically a few hundred micron at the e^+e^- *B*-factories and up to centimeters at the hadron colliders. The decay time in the rest frame of the particle is then obtained from the observed decay length and momentum p in the detector frame,

$$t = \frac{mL}{p}, \qquad (35)$$

where m is the rest mass of the particle. At the e^+e^- *B*-factories the production point is not reconstructed and one measures the difference between the decay time of the "signal" *B* and the "tagging" *B* instead.

The mixing process described above changes the 'flavour' of the meson as a function of its decay time with a frequency governed by Δm . If one can measure both the flavour at the time of production and the flavour at the time of decay, the decay time distributions for 'mixed' (equal flavour) and 'unmixed' (opposite flavour) events are given by Eq. 13. The observed distributions for $B_s^0 \to D_s^+ \pi^-$ decays in an actual experiment – the LHCb experiment at CERN – are shown in Fig. 5. The mixing frequency Δm_s is extracted from the oscillation that modulates the decay time distribution.

The distribution in Fig. 5. differs in several aspects from the function in Eq. 13. First, at small decay times, the exponential shape is distorted by inefficiencies in the event selection. In this particular case, the drop in efficiency at small B decay times arrises from a requirement on the minimum distance between the final state tracks and the primary vertex. This selection was applied in order to remove a large fraction of the prompt (zero lifetime) background in an early stage of the event selection. Though less important for the determination of the mixing frequency, calibration of the decay time acceptance is crucial to obtain an unbiased estimate of the lifetime parameters Γ and $\Delta\Gamma$.

Second, the observed amplitude of the oscillation is much smaller than that expected from Eq. 13. This 'dilution' of the oscillation amplitude is caused by the imperfect determination of the flavour of the initial state and by decay time resolution effects, both of which we now discuss in more detail.

For flavour-specific final states, such as the $B_s^0 \to D_s^+ \pi^-$ decays used for Fig. 5, the flavour at the time of decay follows from the charge of the final state particles:

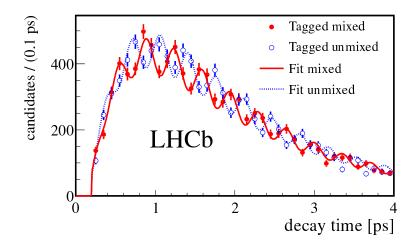


Figure 5: Observed decay time distribution for samples enhanced in 'mixed' and 'unmixed' $B_s^0 \to D_s^+ \pi^-$ and $\overline{B}_s^0 \to D_s^- \pi^+$ candidate decays in 1.0 fb⁻¹ of proton-proton collisions at the LHCb experiment at CERN.³⁶

The charge of the D_s meson (reconstructed in decays to charged kaons and pions) uniquely determines whether the *b* quark was a *b* or an anti-*b*.

The determination of the flavour at the time of the production of the B^0 is performed with a procedure that is called 'flavour tagging'. Two methods of flavour tagging are used. The first method relies on the fact that b quarks are produced in $b\bar{b}$ pairs. Consequently, at the time of production there are two Bhadrons with opposite b flavour in the event. Assuming that the flavour of the other B — called the tag-side or tagging B — can be inferred from its decay products, the initial flavour of the 'signal' B follows. The tagging B is usually not fully reconstructed such that only part of its decay products can be used to identify its flavour. The charge of high p_{\perp} leptons and kaons can be used, as well as the total charge of an inclusively reconstructed vertex. This procedure is called 'opposite-side tagging'. Note that one inherent limitation to this method is that approximately half the tagging B hadrons are neutral mesons and hence subject to flavour oscillations as well, leading to mistakes in the flavour tag.

The second method of flavour tagging exploits that the spectator quark (the s (d) quark for B_s^0 (B_d^0) mesons) also originates from a quark-anti-quark pair, leading to a flavour correlation between the B meson and a light meson close to the B meson in the fragmentation. The algorithm selects a charged kaon (or pion, for B_d^0) that is near in phase space to the B meson. The charge of the kaon, in case of B_s^0 , or the pion, in case of B_d^0 , reveals the sign of the b quark. This procedure is usually referred to as 'same-side tagging'.

Mistakes in flavour tagging lead to a dilution of the observed oscillation asymmetry,

$$A_{\rm mix}^{\rm observed}(t) = D A_{\rm mix}(t).$$
(36)

In practice, the dilution factor D appears in front of all $\sin \Delta mt$ and $\cos \Delta mt$ terms in the differential decay rates, because it is exactly those terms that change sign between the expressions for an initial b or initial anti-b state. The dilution

factor due to flavour tagging is equal to

$$D^{\text{tag}} = 1 - 2w \tag{37}$$

where w is the fraction of events in which the tag is wrong. Flavour tagging performance is expressed as the so-called effective tagging efficiency or tagging power $P = \epsilon_{\text{tag}} D_{\text{tag}}^2$ where ϵ_{tag} is the fraction of events for which a flavour tag could be obtained. Typical values for the tagging power are 30% at the e^+e^- *B*-factories and a few percent at hadron colliders.

Besides the imperfect flavour tagging also the effects of finite decay time resolution lead to a dilution effect. For a Gaussian resolution σ_t the dilution is given by³⁷

$$D^{\text{reso}} = \exp\left(-\frac{1}{2}\sigma_t^2 \Delta m^2\right). \tag{38}$$

The decay time resolution at high-energy machines is in general better than at the *B*-factories due to the larger boost and reduced effects of multiple scattering. The resolution depends on the final state and is substantially worse for partially reconstructed decays than for fully reconstructed decays. For the latter, it ranges from about 0.6 ps at the asymmetric-energy e^+e^- factories down to about 0.05 ps at the LHCb experiment with its forward geometry. With these numbers the resolution dilution factor for B_s^0 oscillations is 0.7 at the latter experiment and negligibly small at the $\Upsilon(4S)$ factories, illustrating why the measurement of Δm_s is the exclusive domain of experiments at high-energy machines.

For measurements of the CP violating phase ϕ_f a proper calibration of dilution factors is essential. The resolution function can be obtained from simulations or by taking a process with a known 'zero' decay time distribution, such as prompt J/ψ production. The flavour tagging performance is calibrated exactly by measuring the size of the amplitude observed in the decay time distribution of flavour-specific final states, such as shown in Fig. 5.

4 Status of experimental constraints on B_s^0 mixing

4.1 Mixing frequency

The first evidence of mixing in neutral B mesons was obtained by the Argus experiment in 1987: by counting the relative fraction of mixing and unmixed events the value of the B_d^0 mixing frequency Δm_d could be extracted using the expression for the integrated oscillation probability in Eq. 14.³⁸ As this was an integrated rate the decay time of the candidates did not need to be reconstructed.

For B_s^0 mesons the oscillation period is so small compared to the lifetime, that the integrated oscillation rate does not provide a meaningful constraint on the mixing frequency. Rather, the measurement of Δm_s is extracted from a fit to the decay time distribution. The first evidence of mixing in B_s^0 mesons was obtained by the CDF experiment in 2006, using a combination of fully reconstructed $B_s^0 \rightarrow$ $D_s^+\pi^-$ and $B_s^0 \rightarrow D_s^+\pi^-\pi^+\pi^-$ and partially reconstructed semi-leptonic $B_s^0 \rightarrow$ $D_s^+ \ell^- \bar{\nu}_\ell X$ decays.³⁹ The current world average value is dominated by the latest LHCb result,

$$\Delta m_s = 17.768 \pm 0.023 \,(\text{stat}) \pm 0.006 \,(\text{syst}) \,[\text{ps}^{-1}] \tag{39}$$

obtained from the decay time distribution of $B_s^0 \to D_s^+ \pi^-$ events shown in Fig. 5.³⁶ The systematic uncertainty is determined by the uncertainties in the length scale and the momentum scale, which enter the measurement of the oscillation frequency through the decay time measurement in Eq. 35.

The current value of Δm_s is in good agreement with the SM predictions presented in section 2. Assuming the validity of the SM, the value of $\Delta m_s/\Delta m_d$ provides the best constraint on V_{ts}/V_{td} .

4.2 Measurements of the mixing phase through time-dependent *CP* violation

Measurements of time-dependent CP violation give access to the mixing phase ϕ_M . The first such measurements were performed by Babar and Belle in the golden mode $B_d^0 \rightarrow J/\psi K_S^{0.40,41}$ Their observation of a large CP violation, in accordance with the prediction in Table 2, established the CKM mechanism of the SM as the dominant source of CP violation in the quark sector.

In the B_s^0 system the best accessible decay channels for this type of measurement are the decays $B_s^0 \to J/\psi\phi(1020)$ (with $\phi(1020) \to K^+K^-$) and $B_s^0 \to J/\psi f^0(980)$ (with $f^0 \to \pi^+\pi^-$). The leading order decay diagrams are shown in Fig. 3. As explained in Section 2, the *CP* violating phase $\phi_s^{c\bar{c}s}$ is extracted from the amplitude of an oscillation in the flavour-tagged decay time distribution. Starting from Eq. 16 and assuming $|\lambda_f| = 1$ the latter takes the form

$$\frac{\mathrm{d}N_{\pm}}{\mathrm{d}t} = N_f \, e^{-\Gamma t} \left[\cosh\left(\frac{1}{2}\Delta\Gamma t\right) - \eta_f \cos\phi_f \sinh\left(\frac{1}{2}\Delta\Gamma t\right) \\ \mp \eta_f \sin\phi_f \sin\left(\Delta m t\right) \right]$$
(40)

where the plus (minus) sign on the left-hand-side holds for mesons produced in a B^0 (\overline{B}^0) flavour eigenstate, ϕ_f was defined in Eq. 25 and η_f is the CP eigenvalue of the final state. Final states with $\eta_f = 1$ are called CP-even, and those with $\eta_f = -1$ are called CP-odd. For $B_s^0 \to J/\psi\phi$ and $B_s^0 \to J/\psi f^0$ the observable phase is usually denoted with the shorthand " ϕ_s ", to distinguish it from the theoretical, tree-level quantity $\phi_s^{c\bar{c}s} = -2\beta_s$.

The $J/\psi f^0(980)$ final state is CP-odd.^{42,43} A recent Dalitz analysis by LHCb has shown that this holds to a good extend for the entire $J/\psi \pi^+\pi^-$ final state.⁴⁴ The phenomenology of the $B_s^0 \to J/\psi \phi(1020)$ decay is more complicated. Since it concerns a decay to two vector mesons (both the J/ψ and the ϕ have spin one) the final state is a superposition of states with different angular momentum quantum numbers, leading to different values of η_f . In order to extract ϕ_s these contributions need to be statistically disentangled using the observed decay angles, requiring a so-called 'time-dependent angular analysis' of the data. Near the $\phi(1020)$ resonance the $B_s^0 \to J/\psi\phi$ final state receives contributions from four amplitudes, namely three P-wave amplitudes that belong to the spinone $\phi \to K^+K^-$ decays and a small S-wave component, that is partially from $f^0(980) \to K^+K^-$.⁴⁵ The total decay time distribution can be written as the sum of 10 equations reminiscent of Eq. 40 above, one for each of the four amplitudes, and another six for their interference terms.

Although the angular analysis certainly makes the analysis of the data more complicated, it also has some notable advantages: First, because of the mixture of odd and even final states, the average observed decay time is sensitive to both $\Gamma_{\rm H}$ and $\Gamma_{\rm L}$ (or, equivalently, Γ and $\Delta\Gamma$). Second, as the interference terms contains flavour-dependent sin Δmt terms with approximately unit amplitude, the decay is to a certain extend self-tagging: In principle one can extract the tagging dilution from the fit to the data without the use of a tagging control channel. In practise, smaller uncertainties are obtained if the tagging dilution is constrained to a control sample. Finally, thanks to these same interference terms, the value of Δm_s can be measured. Note that this allows to extract all mixing parameters from just $B_s^0 \rightarrow J/\psi\phi$ decays alone.

The most precise determination of ϕ_s with $B_s^0 \to J/\psi \phi$ and $B_s^0 \to J/\psi f^0$ events has been reported by LHCb.⁴⁶ The two final states yield compatible values, with uncertainties of about 0.09 and 0.17 respectively. The combined result is

$$\phi_s = 0.01 \pm 0.07 \,(\text{stat}) \pm 0.01 \,(\text{syst}) \,[\text{rad}],$$
(41)

and dominates the current world average. The main contributions to the systematic uncertainty are from the decay angle acceptance for $B_s^0 \to J/\psi\phi$ and from the background model in $B_s^0 \to J/\psi f^0$.

The expression for the partial width Eq. 40 remains invariant under the substitution $(\Delta\Gamma_q, \phi_q) \mapsto (-\Delta\Gamma_q, \pi - \phi_q)$, leaving room for a discrete ambiguity in the result extracted from the data. The SM predicts $\Delta\Gamma_s > 0$ and ϕ_s close to zero. In the expressions for $B_s^0 \to J/\psi\phi$ decays, involving both *P*-wave and *S*-wave amplitudes, the ambiguity persists, but also involves the (strong) phase differences between the amplitudes. In particular, the relative phase between the *P*-wave and *S*-wave amplitude changes sign. Although the relative phase cannot cleanly be predicted, the variation of the phase difference with the K^+K^- invariant mass, which varies rapidly across the $\phi(1020)$ resonance, is well known,⁴⁷ allowing the ambiguity to be resolved.^{48,49} Using this technique measurements by the LHCb collaboration have shown that only the solution with $\Delta\Gamma_s > 0$ and $\phi_s \approx 0$ is viable,⁵⁰ in agreement with the prediction.

4.3 Lifetimes

Constraints on the average lifetime Γ_s and the lifetime difference $\Delta\Gamma_s$ are obtained by combining information from states with different CP content, c.f. Eq. 28. As indicated above the analysis of the vector-vector final state $B_s^0 \rightarrow J/\psi\phi$ allows for the extraction of both Γ_s and $\Delta\Gamma_s$. In the absence of CP violation the lifetime of a CP-odd final decay like $B_s^0 \rightarrow J/\psi f^0$ is $1/\Gamma_{\mathrm{H},s}$, while that of the CP-even final state $B_s^0 \to K^+ K^-$ is $1/\Gamma_{\mathrm{L},s}$. The lifetime measured in flavour specific decays is equal to $1/\Gamma_s \times (4\Gamma_s^2 + \Delta\Gamma_s^2)/(4\Gamma_s^2 - \Delta\Gamma_s^2)$.

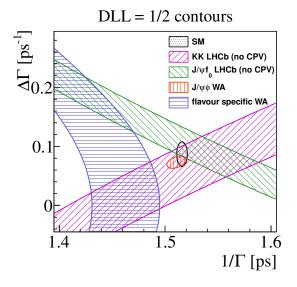


Figure 6: Constraints on $\Delta\Gamma$ and $1/\Gamma_s$ shown as $\Delta \log \mathcal{L}$ contours obtained from the analysis of $B_s^0 \to J/\psi\phi$ decays (author's average from $D0^{51}$, CDF^{52} , $ATLAS^{53}$, CMS^{54} and $LHCb^{46}$), $B_s^0 \to J/\psi f^{0-46}$, $B_s^0 \to K^+K^{-55}$ and the HFAG average for flavour specific decays⁵⁶. The constraints from $B_s^0 \to J/\psi f^0$ and $B_s^0 \to K^+K^$ are obtained under the assumption that there is no CP violation in these decays. The SM prediction (see text) is shown in black.

These different experimental constraints, shown in Fig. 6, are currently in good agreement. The combined average of the $B_s^0 \to J/\psi \phi$ and $B_s^0 \to J/\psi f^0$ results is

$$\Delta\Gamma_s = 0.081 \pm 0.011 \,[\text{ps}^{-1}] 1/\Gamma_s = 1.519 \pm 0.010 \,[\text{ps}]$$
(42)

The SM prediction, using for $\Delta\Gamma$ the value in Tab. 2 and for $\tau(B_s^0)$ the predicted ratio in Eq. 33 and the world average value of $\tau(B_d^0)$, is in good agreement with the measurements. It is noteworthy that the non-zero value of $\Delta\Gamma$ leads to subtleties in the definition of branching fractions, affecting for instance the prediction of the $B_s^0 \to \mu^+\mu^-$ branching fraction by about 10%⁵⁷.

4.4 Flavour-specific asymmetry

Figure 7 summarizes experimental constraints on CP violation in mixing obtained from measurements of the flavour-specific asymmetry $a_{\rm fs}$ (defined in Eq. 20). A measurement of $a_{\rm fs}$ requires both an understanding of the relative production rate of B^0 and \overline{B}^0 and of the relative reconstruction efficiencies for the final states \overline{f} and f.

At the e^+e^- *B*-factories the best constraints in the B_d^0 system have been obtained using same-sign di-lepton events,

$$a_{\rm fs}^d = \frac{\Gamma(\Upsilon(4S) \to \ell^+ \ell^+) - \Gamma(\Upsilon(4S) \to \ell^- \ell^-)}{\Gamma(\Upsilon(4S) \to \ell^+ \ell^+) + \Gamma(\Upsilon(4S) \to \ell^- \ell^-)}.$$
(43)

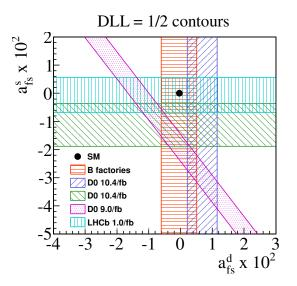


Figure 7: Constraints on on the flavour-specific asymmetry in the B_d^0 and B_s^0 mixing shown as $\Delta \log \mathcal{L}$ contours using data from Babar⁵⁸, Belle⁵⁹, D0^{60,61} and LHCb⁶². The SM prediction is shown in black.

The result, $a_{\rm fs}^d = -0.0005 \pm 0.0056$, from a combination⁵⁶ of BaBar⁵⁸ and Belle⁵⁹ measurements, is perfectly compatible with the expectation. A production asymmetry is not a concern at the *B* factories, but an asymmetry in the efficiency is. This is why these measurements are systematics dominated, even though they have been performed with only a fraction of the *B*-factory data set.

As explained above high statistics measurements in the B_s^0 system can only be performed at high-energy colliders. Two types of probes have been used. In the same-sign di-lepton analysis B_d^0 and B_s^0 decays cannot be distinguished, such that at a high-energy collider one measures a linear combination of the $a_{\rm fs}(B_d^0)$ and $a_{\rm fs}(B_s^0)$,

$$A_{\rm fs}^b = C_d \, a_{\rm fs}^d \, + \, (1 - C_d) \, a_{\rm fs}^s \tag{44}$$

where the coefficient for B_d^0 is approximately $C_d = 0.59$ at the Tevatron⁶³. To reduce the uncertainty from an eventual tracking efficiency asymmetry D0 regularly reverses the magnetic field, a strategy that is also applied by LHCb. Perhaps the most tantalizing sign of physics beyond the SM in B^0 mixing comes from the observation of a non-zero value for this effective asymmetry by the D0 collaboration⁶³, shown by the diagonal band in Fig. 7.

An important concern in the same-sign di-lepton analysis is the understanding of asymmetries in the non-*B* backgrounds, for instance in muons from kaon and pion decays in flight. The purity for the signal can be substantially be improved with a more exclusive reconstruction, that also allows for a separation of the B_d^0 and B_s^0 contribution: the asymmetry in $B_s^0 \to D_s^+ \mu^- \bar{\nu}_{\mu} X$ production has been studied by both D0⁶⁰ and LHCb⁶², while D0 has looked in addition at the $B_d^0 \to D^+ \mu^- \bar{\nu}_{\mu} X$ asymmetry⁶¹.

In these analyses the opposite side b hadron is not tagged, leading to a slightly different relation to $a_{\rm fs}$. Including the effect of an eventual production asymmetry,

defined as

$$a_{\text{prod}} = \frac{N(B^{0}(t=0)) - N(\overline{B}^{0}(t=0))}{N(B^{0}(t=0)) + N(\overline{B}^{0}(t=0))}$$
(45)

the observed asymmetry is related to $a_{\rm fs}$ by

$$\frac{N(D_q^-\mu^+) - N(D_q^+\mu^-)}{N(D_q^-\mu^+) + N(D_q^+\mu^-)} = \frac{a_{\rm fs}}{2} + \left(\frac{a_{\rm fs}}{2} - a_{\rm prod}\right) \frac{\int_0^\infty {\rm d}t \, e^{-\Gamma t} \cos(\Delta m \, t)}{\int_0^\infty {\rm d}t \, e^{-\Gamma t} \cosh(\frac{1}{2}\Delta\Gamma \, t)} \tag{46}$$

At the Tevatron, a proton-anti-proton collider, the production asymmetry is zero. At the LHC it is expected to be at the percent level, but with large uncertainty. As a consequence of the rapid oscillations, the integral on the right hand side of Eq. 46 is of the order of 1 per mille for B_s^0 mesons, which strongly dilutes any contribution from the production asymmetry. This is not the case for B_d^0 mesons and explains why LHCb can measure $a_{\rm fs}^s$ but not $a_{\rm fs}^d$ with this method. As shown in Fig. 7 the semi-exclusive $D_q^+\mu^-$ analyses are competitive with the di-lepton analysis. So far they are in good agreement with the SM.

5 Concluding remarks and Outlook

I have presented a brief review of experimental constraints of mixing phenomena in B_s^0 decays. These phenomena are interesting because they are cleanly predicted in the SM and sensitive to physics at higher mass scales. While mixing in the B_d^0 system has been extensively studied at the e^+e^- *B*-factories, the B_s^0 system is the exclusive domain of high-energy colliders. The Tevatron experiments CDF and D0 have shown the potential of this research, being the first experiments to observe B_s^0 oscillations and rule out leading order new physics effects. The LHC experiments, in particular LHCb, have caught on quickly, providing even stronger constraints on the oscillation frequency, lifetimes and time-dependent *CP* violation.

With only a subset of the data from the first LHC run analysed, and more luminosity expected in 2015 and beyond, we can expect significantly tighter constraints in the near future. The increase in available statistics also allows the study of mixing-induced CP violation in more decay modes, such as $B_s^0 \to \phi \phi^{64}$, $B_s^0 \to h^+ h^-$ and $B_s^0 \to D^{(*)} \overline{D}^{(*)}$. Clearly, as statistical precision increases, controlling systematic uncertainties, both experimental and theoretical, becomes more important. Experimental uncertainties in lifetime and a_{fs}^s are expected to be dominated by detector effects rather soon. On the other hand, combinations of CP violation and branching fraction measurements for different channels, will help to reduce theoretical uncertainties due to subdominant amplitudes and nonperturbative effects.

Finally, we can expect another jump in precision near the end of the decade. The upgrade of the KEKB accelerator and Belle detector are well under way, with the start of data taking planned for 2015⁶⁵. The LHCb collaboration is preparing an upgrade that allows for a 10-fold increase in integrated luminosity, to be collected in a five year period starting approximately in 2019⁶⁶. These flavour physics facilities are both competitive with and complementary to the direct searches for new forces and particles in high energy collisions.

Acknowledgments

The author is grateful to Prof. Dr. Gerhard Raven and Prof. Dr. Robert Fleischer for proofreading the manuscript and providing many useful suggestions. The author receives funding from the Netherlands organisation for scientific research (NWO/FOM) through the VIDI scheme.

References

- M. Kobayashi and T. Maskawa, CP Violation in the Renormalizable Theory of Weak Interaction, Prog. Theor. Phys. 49 (1973) 652.
- [2] Particle Data Group, J. Beringer et al., Review of particle physics, Phys. Rev. D 86 (2012) 010001.
- [3] S. Glashow, J. Iliopoulos, and L. Maiani, Weak Interactions with Lepton-Hadron Symmetry, Phys. Rev. D2 (1970) 1285.
- [4] G. C. Branco, L. Lavoura, and J. P. Silva, *CP violation*, Int. Ser. Monogr. Phys. **103** (1999) 1; I. I. Bigi and A. Sanda, *CP violation*, Camb. Monogr. Part. Phys. Nucl. Phys. Cosmol. **9** (2000) 1.
- [5] R. Fleischer, CP violation in the B system and relations to $K \to \pi \nu \bar{n} u$ decays, Phys. Rept. **370** (2002) 537, arXiv:hep-ph/0207108.
- [6] A. Lenz, Theoretical update of B-Mixing and Lifetimes, arXiv:1205.1444.
- [7] U. Nierste, Three Lectures on Meson Mixing and CKM phenomenology, arXiv:0904.1869.
- [8] A. J. Buras, Flavor physics and CP violation, arXiv:hep-ph/0505175;
 Y. Nir, Flavour physics and CP violation, arXiv:1010.2666;
 Y. Grossman, Introduction to flavor physics, arXiv:1006.3534;
 G. Isidori, Flavor physics and CP violation, arXiv:1302.0661.
- [9] O. Schneider, $B^0 \overline{B}^0$ mixing, in Review of Particle Physics, vol. 86, pp. 1066–1071. American Physical Society, Jul, 2012. doi: 10.1103/Phys-RevD.86.010001.
- [10] I. Dunietz, R. Fleischer, and U. Nierste, In pursuit of new physics with B⁰_s decays, Phys. Rev. D63 (2001) 114015, arXiv:hep-ph/0012219.
- [11] A. B. Carter and A. Sanda, CP Violation in B Meson Decays, Phys. Rev. D23 (1981) 1567; I. I. Bigi and A. Sanda, Notes on the Observability of CP Violations in B Decays, Nucl. Phys. B193 (1981) 85.
- [12] C. Dib, I. Dunietz, F. J. Gilman, and Y. Nir, Standard Model Predictions for CP Violation in B⁰ Meson Decay, Phys. Rev. D41 (1990) 1522.

- [13] R. Fleischer and R. Knegjens, Effective Lifetimes of B_s Decays and their Constraints on the B_s⁰-B_s⁰ Mixing Parameters, Eur. Phys. J. C71 (2011) 1789, arXiv:1109.5115.
- [14] M. Beneke, G. Buchalla, and I. Dunietz, Width Difference in the B_s⁰ B_s⁰ System, Phys. Rev. D54 (1996) 4419, arXiv:hep-ph/9605259; M. Beneke et al., Next-to-leading order QCD corrections to the lifetime difference of B(s) mesons, Phys. Lett. B459 (1999) 631, arXiv:hep-ph/9808385; M. Beneke, G. Buchalla, A. Lenz, and U. Nierste, CP asymmetry in flavor specific B decays beyond leading logarithms, Phys. Lett. B576 (2003) 173, arXiv:hep-ph/0307344.
- [15] M. Ciuchini et al., Lifetime differences and CP violation parameters of neutral B mesons at the next-to-leading order in QCD, JHEP 0308 (2003) 031, arXiv:hep-ph/0308029.
- [16] A. Lenz and U. Nierste, Theoretical update of $B_s^0 \overline{B}_s^0$ mixing, JHEP **06** (2007) 072, arXiv:hep-ph/0612167.
- [17] A. Badin, F. Gabbiani, and A. A. Petrov, Lifetime difference in B_s mixing: Standard model and beyond, Phys. Lett. B653 (2007) 230, arXiv:0707.0294.
- [18] A. Lenz and U. Nierste, Numerical updates of lifetimes and mixing parameters of B mesons, arXiv:1102.4274.
- [19] T. Inami and C. Lim, Effects of Superheavy Quarks and Leptons in Low-Energy Weak Processes $K_L \to \mu \bar{\mu}, K^+ \to \pi^+ \nu \bar{\nu}$ and $K^0 \leftrightarrow \bar{K}^0$, Prog. Theor. Phys. **65** (1981) 297.
- [20] C. Tarantino, Flavor Lattice QCD in the Precision Era, arXiv:1210.0474.
- [21] A. Buras, W. Slominski, and H. Steger, B⁰-B
 ⁰ Mixing, CP Violation and the B Meson Decay, Nucl. Phys. B245 (1984) 369.
- [22] CKMfitter Group, J. Charles et al., CP violation and the CKM matrix: Assessing the impact of the asymmetric B factories, Eur. Phys. J. C41 (2005) 1, arXiv:hep-ph/0406184; J. Charles et al., Predictions of selected flavour observables within the Standard Model, Phys. Rev. D84 (2011) 033005, arXiv:1106.4041.
- [23] M. Ciuchini et al., 2000 CKM triangle analysis: A Critical review with updated experimental inputs and theoretical parameters, JHEP 0107 (2001) 013, arXiv:hep-ph/0012308; UTfit Collaboration, M. Bona et al., Modelindependent constraints on Δ F=2 operators and the scale of new physics, JHEP 0803 (2008) 049, arXiv:0707.0636.
- [24] A. Lenz et al., Anatomy of new physics in $B-\overline{B}$ mixing, Phys. Rev. D83 (2011) 036004, arXiv:1008.1593.

- [25] J. Laiho, E. Lunghi, and R. S. Van de Water, Lattice QCD inputs to the CKM unitarity triangle analysis, Phys. Rev. D81 (2010) 034503, arXiv:0910.2928;
 A. Bazavov et al., Neutral B-meson mixing from three-flavor lattice QCD: Determination of the SU(3)-breaking ratio ξ, Phys. Rev. D86 (2012) 034503, arXiv:1205.7013; ETM collaboration, N. Carrasco et al., Neutral meson oscillations in the Standard Model and beyond from Nf=2 Twisted Mass Lattice QCD, PoS LATTICE2012 (2012) 105, arXiv:1211.0565.
- [26] M. Neubert and C. T. Sachrajda, Spectator effects in inclusive decays of beauty hadrons, Nucl. Phys. B483 (1997) 339, arXiv:hep-ph/9603202.
- [27] F. Gabbiani, A. I. Onishchenko, and A. A. Petrov, Spectator effects and lifetimes of heavy hadrons, Phys. Rev. D70 (2004) 094031, arXiv:hep-ph/0407004.
- [28] R. Fleischer, Extracting γ from $B(s/d) \rightarrow J/\psi K_S$ and $B(d/s) \rightarrow$ $D^+(d/s)D^-(d/s)$, Eur. Phys. J. C10 (1999) 299, arXiv:hep-ph/9903455; M. Ciuchini, M. Pierini, and L. Silvestrini, The Effect of penguins in the $B_d^0 \rightarrow J/\psi K^0 CP$ asymmetry, Phys. Rev. Lett. **95** (2005) 221804, arXiv:hep-ph/0507290; S. Faller, M. Jung, R. Fleischer, and T. Mannel, The Golden Modes $B^0 \to J/\psi K(S,L)$ in the Era of Precision Flavour Physics, Phys. Rev. D79 (2009) 014030, arXiv:0809.0842; S. Faller, R. Fleischer, and T. Mannel, Precision physics with $B_s^0 \to J/\psi\phi$ at the LHC: the quest for new physics, Phys. Rev. D79 (2009) 014005, arXiv:0810.4248; C.-W. Chiang et al., New physics in $B_s^0 \to J/\psi\phi$: a general analysis, JHEP **1004** (2010) 031, arXiv:0910.2929; K. De Bruyn, R. Fleischer, and P. Koppenburg, Extracting γ and Penguin Topologies through CP Violation in $B_s^0 \to J/\psi K_S^0$, Eur. Phys. J. C70 (2010) 1025, arXiv:1010.0089; M. Ciuchini, M. Pierini, and L. Silvestrini, Theoretical uncertainty in sin 2β : An Update, arXiv:1102.0392; R. Fleischer, Penguin Effects in $\phi_{d,s}$ Determinations, arXiv:1212.2792; B. Bhattacharya, A. Datta, and D. London, Reducing Penquin Pollution, Int. J. Mod. Phys. A28 (2013) 1350063, arXiv:1209.1413.
- [29] A. J. Buras, Minimal flavour violation and beyond: Towards a flavour code for short distance dynamics, Acta Phys. Polon. B41 (2010) 2487, arXiv:1012.1447.
- [30] Y. Grossman, Y. Nir, and M. P. Worah, A Model independent construction of the unitarity triangle, Phys. Lett. B407 (1997) 307, arXiv:hep-ph/9704287.
- [31] P. Ball and R. Fleischer, *Probing new physics through B mixing:* Status, benchmarks and prospects, Eur. Phys. J. C48 (2006) 413, arXiv:hep-ph/0604249.
- [32] A. Lenz et al., Constraints on new physics in B-B mixing in the light of recent LHCb data, Phys. Rev. D86 (2012) 033008, arXiv:1203.0238.
- [33] A. J. Buras, F. De Fazio, J. Girrbach, and M. V. Carlucci, *The Anatomy of Quark Flavour Observables in 331 Models in the Flavour Precision Era*, JHEP **1302** (2013) 023, arXiv:1211.1237.

- [34] LHCb Collaboration, R. Aaij et al., Implications of LHCb measurements and future prospects, Eur. Phys. J. C73 (2013) 2373, arXiv:1208.3355.
- [35] S. Herb et al., Observation of a Dimuon Resonance at 9.5-GeV in 400-GeV Proton-Nucleus Collisions, Phys. Rev. Lett. 39 (1977) 252.
- [36] LHCb collaboration, R. Aaij et al., Precision measurement of the $B_s^0 \overline{B}_s^0$ oscillation frequency with the decay $B_s^0 \to D_s^- \pi^+$, New J. Phys. **15** (2013) 053021, arXiv:1304.4741.
- [37] H. G. Moser and A. Roussarie, Mathematical methods for $B^0 \cdot \overline{B}^0$ oscillation analyses, Nucl. Instrum. Meth. **A384** (1997) 491.
- [38] Argus Collaboration, H. Albrecht *et al.*, Observation of $B^0 \overline{B}^0$ Mixing, Phys. Lett. **B192** (1987) 245.
- [39] CDF Collaboration, A. Abulencia et al., Measurement of the B⁰_s B⁰_s Oscillation Frequency, Phys. Rev. Lett. 97 (2006) 062003, arXiv:hep-ex/0606027.
- [40] BABAR, B. Aubert et al., Observation of CP violation in the B⁰ meson system, Phys. Rev. Lett. 87 (2001) 091801, arXiv:hep-ex/0107013.
- [41] Belle, K. Abe et al., Observation of large CP violation in the neutral B meson system, Phys. Rev. Lett. 87 (2001) 091802, arXiv:hep-ex/0107061.
- [42] S. Stone and L. Zhang, S-waves and the measurement of CP violating phases in B⁰_s decays, Phys. Rev. D79 (2009) 074024, arXiv:0812.2832.
- [43] R. Fleischer, R. Knegjens, and G. Ricciardi, Anatomy of $B_{s,d}^0 \rightarrow J/\psi f_0(980)$, Eur. Phys. J. C71 (2011) 1832, arXiv:1109.1112.
- [44] LHCb Collaboration, R. Aaij *et al.*, Analysis of the resonant components in $B_s^0 \to J/\psi \pi^+ \pi^-$, Phys. Rev. **D86** (2012) 052006, arXiv:1204.5643.
- [45] LHCb Collaboration, R. Aaij et al., Amplitude analysis and the branching fraction measurement of $\overline{B}_s^0 \to J/\psi K^+ K^-$, Phys. Rev. **D87** (2013) 072004, arXiv:1302.1213.
- [46] LHCb collaboration, R. Aaij et al., Measurement of CP violation and the B_s^0 meson decay width difference with $B_s^0 \to J/\psi K^+ K^-$ and $B_s^0 \to J/\psi \pi^+ \pi^$ decays, Phys. Rev. D 87, **112010** (2013), arXiv:1304.2600.
- [47] E. P. Wigner, Lower Limit for the Energy Derivative of the Scattering Phase Shift, Phys. Rev. 98 (1955) 145.
- [48] BaBar Collaboration, B. Aubert *et al.*, Ambiguity-free measurement of $\cos(2\beta)$: Time-integrated and time-dependent angular analyses of $B \rightarrow J/\psi K\pi$, Phys. Rev. **D71** (2005) 032005, arXiv:hep-ex/0411016.

- [49] Y. Xie, P. Clarke, G. Cowan, and F. Muheim, Determination of $2\beta_s$ in $B_s \rightarrow J/\psi K^+K^-$ decays in the presence of a K^+K^- S-Wave contribution, JHEP **09** (2009) 074, arXiv:0908.3627.
- [50] LHCb Collaboration, R. Aaij et al., Determination of the sign of the decay width difference in the B_s system, Phys. Rev. Lett. 108 (2012) 241801, arXiv:1202.4717.
- [51] D0 Collaboration, V. M. Abazov *et al.*, Measurement of the CP-violating phase $\phi_s^{J/\psi\phi}$ using the flavor-tagged decay $B_s^0 \to J/\psi\phi$ in 8 fb⁻¹ of $p\bar{p}$ collisions, Phys. Rev. **D85** (2012) 032006, arXiv:1109.3166.
- [52] CDF Collaboration, T. Aaltonen et al., Measurement of the Bottom-Strange Meson Mixing Phase in the Full CDF Data Set, Phys. Rev. Lett. 109 (2012) 171802, arXiv:1208.2967.
- [53] ATLAS Collaboration, G. Aad et al., Time-dependent angular analysis of the decay $B_s^0 \to J/\psi\phi$ and extraction of $\Delta\Gamma_s$ and the CP-violating weak phase ϕ_s by ATLAS, JHEP **1212** (2012) 072, arXiv:1208.0572.
- [54] CMS Collaboration, S. Chatrchyan *et al.*, Measurement of the B_s^0 lifetime difference, CMS-PAS-BPH-11-006, 2012.
- [55] LHCb Collaboration, R. Aaij *et al.*, Measurement of the effective $B_s^0 \rightarrow K^+K^-$ lifetime, Phys. Lett. **B716** (2012) 393, arXiv:1207.5993.
- [56] Heavy Flavor Averaging Group, Y. Amhis et al., Averages of B-Hadron, C-Hadron, and tau-lepton properties as of early 2012, arXiv:1207.1158.
- [57] K. De Bruyn et al., Branching Ratio Measurements of B_s Decays, Phys. Rev. **D86** (2012) 014027, arXiv:1204.1735; K. De Bruyn et al., Probing New Physics via the $B_s^0 \rightarrow \mu^+\mu^-$ Effective Lifetime, Phys. Rev. Lett. **109** (2012) 041801, arXiv:1204.1737.
- [58] BABAR Collaboration, B. Aubert et al., Search for T, CP and CPT violation in B⁰-B
 ⁰ Mixing with inclusive dilepton events, Phys. Rev. Lett. 96 (2006) 251802, arXiv:hep-ex/0603053.
- [59] Belle Collaboration, E. Nakano *et al.*, Charge asymmetry of samesign dileptons in $B^0 - \overline{B}^0$ mixing, Phys. Rev. **D73** (2006) 112002, arXiv:hep-ex/0505017.
- [60] D0 Collaboration, V. Abazov *et al.*, Measurement of the semileptonic charge asymmetry using $B_s^0 \to D_s \mu X$ decays, Phys. Rev. Lett. **110** (2013) 011801, arXiv:1207.1769.
- [61] D0 Collaboration, V. M. Abazov et al., Measurement of the semileptonic charge asymmetry in B⁰ meson mixing with the D0 detector, Phys. Rev. D86 (2012) 072009, arXiv:1208.5813.

- [62] LHCb collaboration, R. Aaij *et al.*, Measurement of the flavour-specific CPviolating asymmetry a_{sl}^s in B_s^0 decays, arXiv:1308.1048, Submitted to Phys. Lett. B.
- [63] D0 Collaboration, V. M. Abazov et al., Measurement of the anomalous likesign dimuon charge asymmetry with 9 fb⁻¹ of pp̄ collisions, Phys. Rev. D84 (2011) 052007, arXiv:1106.6308.
- [64] LHCb collaboration, R. Aaij *et al.*, First measurement of the CP-violating phase in $B_s^0 \rightarrow \phi \phi$ decays, Phys. Rev. Lett. 110, **241802** (2013), arXiv:1303.7125.
- [65] Belle II Collaboration, T. Abe, *Belle II Technical Design Report*, arXiv:1011.0352.
- [66] LHCb Collaboration, R. Aaij et al., Framework TDR for the LHCb Upgrade: Technical Design Report, CERN-LHCC-2012-007. LHCb-TDR-12.